Spectral imaging and linear un-mixing enables improved FRET efficiency with a novel GFP2–YFP FRET pair

Timo Zimmermann[a,b], Jens Rietdorf[a,b], Andreas Girod[a,b], Virginie Georget[b], Rainer Pepperkok[a,b,*]

[a] *Advanced Light Microscopy Facility, European Molecular Biology Laboratory, Meyerhofstr. 1, D-69117 Heidelberg, Germany*
[b] *Cell Biology/Cell Biophysics Programme, European Molecular Biology Laboratory, Meyerhofstr. 1, D-69117 Heidelberg, Germany*

Received 7 August 2002; revised 25 September 2002; accepted 26 September 2002

First published online 15 October 2002

Edited by Felix Wieland

Abstract Spectral variants of the green fluorescent protein (GFP) have been extensively used as reporters to image molecular interactions in living cells by fluorescence resonance energy transfer (FRET). However, those GFP variants which are the most efficient donor acceptor pairs for FRET measurements show a high degree of spectral overlap which has hampered in the past their use in FRET applications. Here we use spectral imaging and subsequent un-mixing to quantitatively separate highly overlapping donor and acceptor emissions in FRET measurements. We demonstrate the method in fixed and living cells using a novel GFP based FRET pair (GFP2–YFP (yellow)), which has an increased FRET efficiency compared to the most commonly used FRET pair consisting of cyan fluorescent protein and YFP. Moreover, GFP2 has its excitation maximum at 396 nm at which the YFP acceptor is excited only below the detection level and thus this FRET pair is ideal for applications involving sensitized emission.

Key words: Fluorescence resonance energy transfer; Green fluorescent protein; Protein–protein interaction

1. Introduction

Fluorescence resonance energy transfer (FRET) [1] between spectral variants of the green fluorescent protein (GFP) [2,3] has been extensively used as a method to image molecular processes in living cells such as protein–protein interactions [4] or protease [5] and kinase [6] activities. The FRET efficiency and thus sensitivity in these applications has however been limited by at least two problems. Firstly, due to the spectral overlap of donor and acceptor excitation/emission the acceptor is often also excited directly by the donor excitation, which requires extensive corrections in order to determine FRET by sensitized emission [7]. Secondly, GFP pairs that can be spectrally well separated such as the enhanced blue fluorescent protein (EBFP) and the yellow fluorescent protein (YFP) show very little overlap of donor emission and acceptor excitation and thus have low FRET efficiencies. In contrast, those GFP variants with a high spectral overlap, resulting in a high FRET efficiency, are difficult to separate spectrally by currently available intensity based methods using optical filters. Here we describe an approach that overcomes these limitations.

2. Materials and methods

2.1. Expression plasmids, protein expression and purification

EYFP (Clontech, Heidelberg, Germany) was amplified by PCR generating a 5′-*Bam*HI site and a 3′-*Eco*RI–Stop–*Xho*I site and subcloned (*Bam*HI/*Xho*I) into pcDNA3.1+ (Invitrogen GmbH, Karlsruhe, Germany).

GFP2 (Perkin Elmer, Inc., Dreieich, Germany) is a GFP variant with excitation and emission spectra comparable to the wild-type GFP but with a F64L substitution that increases the brightness significantly (Patent no. US 6,172,188 B1).

For eukaryotic expression, enhanced cyan fluorescent protein (ECFP; Clontech, Heidelberg, Germany) and GFP2 were PCR amplified generating a 5′-*Kpn*I site and a 3′-linker (coding for GGTG) followed by a *Bam*HI site. Subsequently, the *Kpn*I/*Bam*HI-fragments were subcloned into pcDNA-EYFP, generating ECFP–linker–EYFP and GFP2–linker–EYFP tandem constructs.

For expression in mammalian cells, HeLa cells were grown on glass bottom dishes (3.5 cm, MatTek, Ashland, MD, USA). The transfections with the fluorescent protein coding eukaryotic expression vectors using FuGENE6 transfection reagent (Roche, Mannheim, Germany) were performed as described [8]. Unless stated otherwise, cells were fixed with 3.5% paraformaldehyde in PBS for 20 min at room temperature. For the co-localization experiment a PTK2 cell line stably expressing tubulin–YFP was transfected with DNA coding for a GFP-tagged nuclear localization sequence.

For bacterial expression, ECFP, EGFP, EYFP (Clontech) and GFP2 were PCR amplified generating a 5′-*Nde*I site and a 3′-*Eco*RI site and genetically fused to a His6-Tag by subcloning (*Nde*I/*Eco*RI) into pET28b (Novagen, Madison, WI, USA). The expression was performed as described [9]. The purification of the His6-tagged fluorescent proteins using Ni^{2+}-NTA-agarose beads (Qiagen, Hilden, Germany) under native conditions was performed according the manufacturer's instructions. After purification the proteins were dialyzed against PBS buffer.

2.2. Acquisition of fluorescence spectra and calculation of FRET efficiencies

The excitation and emission spectra of the fluorescent proteins were acquired in PBS in 50 μl volumes with a QM-2000-6 spectrofluorometer (Photon Technology International, Lawrenceville, NJ, USA). Extinction coefficients and quantum yields of ECFP, EGFP and EYFP were taken from ref. [10]. The extinction coefficient ε and quantum efficiency Q of GFP2 were determined according to ref. [11] using EGFP as a reference.

The spectral overlap integrals of CFP–YFP and GFP2–YFP were calculated according to the following formula [12]:

$$J(\lambda) = \int_0^\infty \varepsilon(\lambda) f(\lambda) \lambda^4 \mathrm{d}\lambda \quad (1)$$

*Corresponding author.
E-mail address: pepperko@embl-heidelberg.de (R. Pepperkok).

0014-5793/02/$22.00
PII: S0014-5793(02)03508-1

where $J(\lambda)$ is the overlap integral, ε the extinction coefficient of YFP, f the normalized emission spectrum of the donor and λ the wavelength. Overlap integrals in the text are given as percentages of the maximum value possible, e.g. when the donor emission is identical with the YFP excitation spectrum.

The Förster distances R_0 of CFP–YFP and GFP2–YFP were calculated according to the formula [11]:

$$R_0 = 0.211[\kappa^2 n^{-4}\, Q_D J(\lambda)]^{1/6}\ (\text{in Å}) \quad (2)$$

where κ is the orientation factor representing the directions of the emission dipole of the donor and the absorption dipole of the acceptor (κ^2 assumed as 2/3), n is the refractive index of the medium (1.33 for water) and Q_D is the quantum efficiency of the donor.

Finally the FRET efficiency (E) was then calculated as [11]:

$$E = \frac{R_0^6}{R_0^6 + r^6} \quad (3)$$

where r is the distance between donor and acceptor.

2.3. Spectral imaging and linear un-mixing

All imaging experiments were performed on a Leica SP2 confocal microscope (Leica Microsystems, Germany) equipped with an acousto-optical beamsplitter, an 100 mW argon laser (457 nm, 476 nm, 488 nm, 514 nm) and a 20 mW blue diode laser for 405 nm excitation. The four fluorescence detection channels (Ch) were set to the following ranges: Ch 1: 465–485 nm, Ch 2: 490–510 nm, Ch 3: 520–540 nm, Ch 4: 545–565 nm. Settings for gain and offset of the detectors were identical for all experiments to keep the relative contribution of the

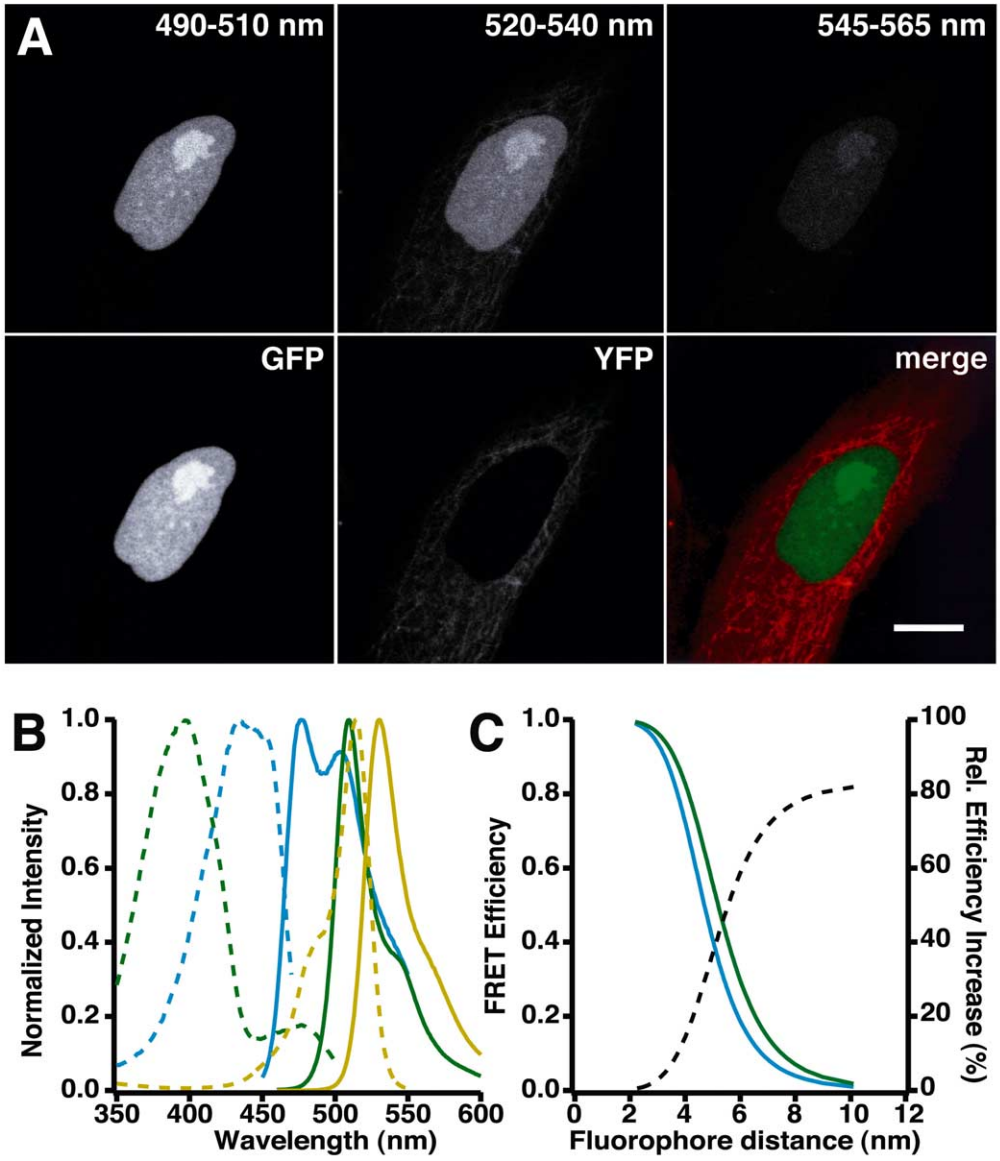

Fig. 1. A: Spectral imaging and linear un-mixing of two GFP variants. Upper row: Fluorescence emitted by living Ptk2 cells expressing nuclear GFP and YFP–tubulin was recorded into four channels as described in Section 2. Shown are the signals in channels 2 to 4. The signal in channel 1 (465–485 nm) is not shown in this particular experiment, since there was no significant contribution to this channel by the GFP or YFP. Lower row: The contributions of the fluorophores into the channels were separated by linear un-mixing and are shown as a GFP, YFP and dual color image. B: Normalized spectra of the excitation (dashed line) and the emission (solid line) of GFP2 (green), CFP (blue) and YFP (yellow). C: FRET efficiencies of the GFP2–YFP and CFP–YFP pairs derived from the spectral properties of the fluorescent proteins as described in Section 2. FRET efficiencies for GFP2–YFP (green) and CFP–YFP (blue) are plotted as a function of the distance between the fluorescent proteins. Efficiencies at any distance are higher for GFP2–YFP than for CFP–YFP. The dotted line shows the relative increase in FRET efficiency for GFP2–YFP as compared to CFP–YFP. Scale bar = 10 μm.

fluorophores to the detection channels constant for spectral un-mixing.

The contributions of the GFP variants CFP, GFP, GFP2 and YFP to each of the four detection channels (spectral signature) were measured in experiments with cells expressing only one of these proteins and normalized to the sum of the signal obtained in the four detection channels (e.g. for CFP: 0.36, 0.33, 0.19, 0.12).

2.3.1. Linear un-mixing. In order to determine the fluorescence emitted by each of two individual fluorophores (FluoA, FluoB) in co-localization or FRET experiments the following formula was applied for every image pixel i:

$$Q(i) = \frac{\mathrm{Ch_x}(i)}{\mathrm{Ch_y}(i)},\ R(i) = \frac{\mathrm{FluoA}(i)}{\mathrm{FluoB}(i)} = \frac{B_y Q(i) - B_x}{A_x - A_y Q(i)}$$

where $\mathrm{Ch_{x,y}}$ represent the signals in detection channels x and y, and A_x, B_x and A_y, B_y the normalized contributions of FluoA or FluoB to channels x and y as they are known from the spectral signatures of the fluorescent proteins.

FluoA and FluoB are then calculated by:

$$\mathrm{FluoA}(i) = \frac{S(i)}{1 + \frac{1}{R(i)}}$$

and

$$\mathrm{FluoB}(i) = \frac{S(i)}{1 + R(i)}$$

with

$$S(i) = \sum_{k=1}^{n} \mathrm{Ch}_k(i).$$

Only two detection channels are necessary for the determination of FluoA and FluoB. However, using four channels, up to six ratios of different channels (e.g. $\mathrm{Ch_1/Ch_2}$, $\mathrm{Ch_1/Ch_3}$, $\mathrm{Ch_1/Ch_4}$) can be calculated and used to determine FluoA and FluoB. The channels with the best signal to noise ratios were selected for un-mixing. For the experiments described here, the ratios $\mathrm{Ch_1/Ch_3}$ and $\mathrm{Ch_1/Ch_4}$ were used for un-mixing CFP–YFP and $\mathrm{Ch_2/Ch_3}$, $\mathrm{Ch_2/Ch_4}$ for GFP2–YFP. The average of the resulting two respective ratios R (see above) was then used to determine FluoA and FluoB.

2.4. Calculation of FRET efficiencies in acceptor photo-bleaching experiments

Acceptor photo-bleaching was performed as described in the legend to Fig. 2. In all experiments the acceptor was bleached to 100%, that is to levels that were indistinguishable from background fluorescence of non-transfected neighboring cells.

Apparent FRET efficiencies E_A in acceptor photo-bleaching experiments were calculated for each pixel i according to formula [13]:

$$E_A(i) = 1 - \frac{F^D(i)}{F^D_{pb}(i)} = E \cdot \alpha_D(i) \cdot \beta \quad (4)$$

F^D represents the emitted donor fluorescence before and F^D_{pb} after photo-bleaching of the acceptor. α is the fraction of donor molecules interacting with acceptor. β is the amount of acceptor that has been photo-bleached relative to the initial acceptor fluorescence before photo-bleaching (100% in all our experiments here). Because of the tandem FRET constructs used in the experiments α can be set to 1. The measured FRET efficiency is therefore equal to the real FRET efficiency.

3. Results and discussion

The high absorption (84 000 M^{-1} cm^{-1}) and quantum yield of YFP [10] ($Q = 0.61$) make it or its improved variants [14] an attractive FRET acceptor. However, it has limitations in its

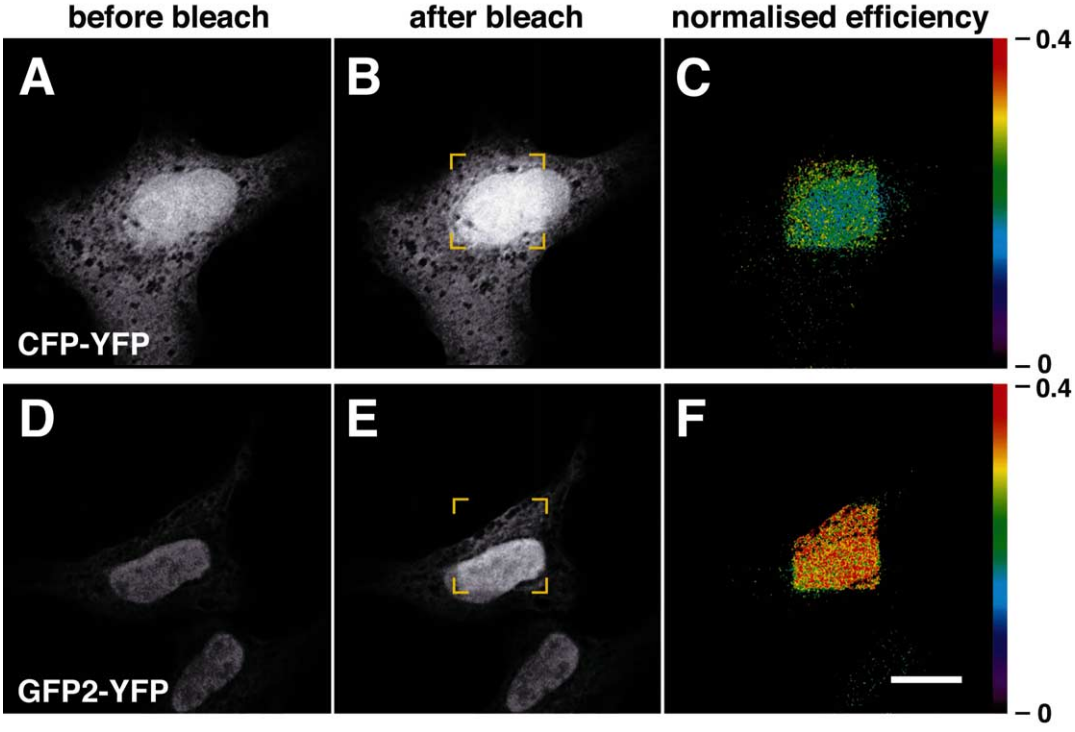

Fig. 2. Imaging FRET efficiencies of the CFP–YFP and GFP2–YFP tandem constructs by acceptor photo-bleaching [17]. HeLa cells were transfected with either CFP–YFP (A–C) or GFP2–YFP (D–F) tandem constructs and fixed 16 h thereafter. Images of the donor before (A,D) and after photo-bleaching (B,E) of the YFP acceptor in a central square of the image view (indicated in B,E) were obtained by spectral imaging and subsequent linear un-mixing as it is described in Section 2. Inside the bleached region the donor is unquenched resulting in an intensity increase indicative of FRET (B,E). False color representations of the FRET efficiencies, calculated according to Eq. 4 in Section 2, are shown in C and F. Scale bar = 10 μm.

use in combination with optimal donors such as EGFP or GFP2. Due to the short Stokes shift of the YFP, donor and YFP emission spectra typically show significant overlap (Fig. 1B), which makes it difficult to separate and quantify the emitted light of the donor and the acceptor.

In order to overcome this problem we have exploited the method of spectral imaging and subsequent linear un-mixing, which uses the signatures of the emission spectra of two or more distinct fluorophores to determine their individual contributions to the sum of the overlapping emitted light in co-localization experiments [15,16]. For this, individual spectral GFP variants were expressed in cells and four images were acquired simultaneously on a confocal microscope with each image channel detecting a 20 nm bandwidth (for details see Section 2). Subsequently, the relative contribution of the emitted light of the GFP variant to each of the four channels was determined, which defined its spectral signature. These signatures were then used in subsequent experiments to determine the fluorescence emitted by each GFP variant in co-localization (Fig. 1) or FRET experiments (Figs. 2 and 3). Fig. 1A demonstrates spectral un-mixing in co-localization experiments using a nuclear GFP and YFP-tagged tubulin. Similar efficiencies in un-mixing were obtained in co-localization experiments involving even three fluorescent proteins such as CFP-, GFP- and YFP-tagged proteins (not shown).

In order to test the usefulness of spectral un-mixing for FRET measurements we generated two GFP based donor/acceptor pairs connected each by an identical linker (tandem constructs). One of the pairs consisted of the commonly used donor/acceptor pair CFP and YFP and the other one of GFP2 and YFP. GFP2 has a higher quantum efficiency ($Q = 0.55$) compared to CFP ($Q = 0.4$) and a larger overlap integral with the YFP acceptor (66% for CFP–YFP and 87% for GFP2–YFP). The GFP2–YFP FRET pair is therefore predicted to have a higher FRET efficiency compared to the CFP–YFP pair, which becomes more pronounced at longer distances between the donor and the acceptor (Fig. 1C). The GFP2–YFP pair has the additional advantage that the GFP2 donor has its excitation maximum at 396 nm, like wild-type GFP, and can therefore be very efficiently excited with a 405 nm diode laser. At this wavelength the direct excitation of the YFP is below 1% of its maximum at 514 nm and below the detection limit of the confocal microscope under the experimental conditions used (see Fig. 3B). In contrast, at 457 nm or 430 nm, typically used for CFP excitation, YFP is directly excited at 10 or 2% of its maximum, respectively. Direct excitation of the acceptor by the donor excitation light complicates quantitative FRET measurements by using the sensitized emission method and a number of independent control measurements have to be introduced to reliably determine FRET [7]. Such corrections are not necessary using GFP2 as a donor together with a 405 nm laser diode as excitation light source. However, since GFP2 and YFP emissions significantly overlap and are thus almost impossible to separate by optical methods using glass filters, quantitative FRET measurements become difficult. This latter problem can be over-come by spectral imaging and subsequent spectral un-mixing.

To demonstrate experimentally the considerations described

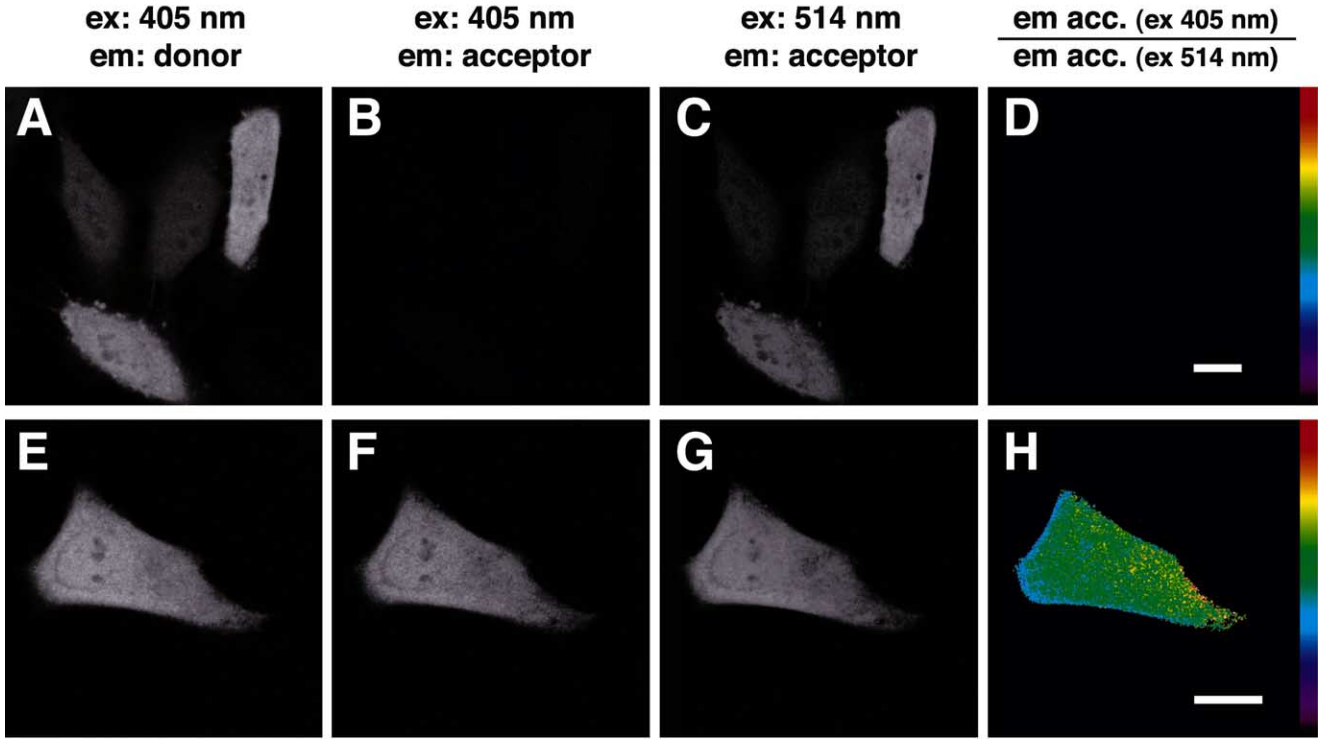

Fig. 3. Imaging of FRET by sensitized emission in living cells. HeLa cells were double-transfected with GFP2 and YFP (A–D) or with the GFP2–YFP tandem construct (E–H) and imaged 16 h thereafter at room temperature. All images shown were acquired by spectral imaging and linear un-mixing as described in Section 2. First, cells were excited at 405 nm and donor (A,E) and acceptor (B,F) emission was determined. Acceptor specific fluorescence upon donor excitation was not detectable in cells co-expressing GFP2 and YFP (B), but a significant signal, indicative of sensitized emission, was obtained in cells expressing the GFP2–YFP tandem construct (F). Thereafter, cells were excited at 514 nm in order to determine the amount of YFP present in the sample (C,G). A false color representation of sensitized emission (B,F) normalized to the acceptor specific fluorescence (C,G) is shown in D and H. Scale bar = 10 μm.

above, cells were transfected with the tandem constructs and FRET efficiencies were imaged in fixed cells by acceptor photo-bleaching [17] (Fig. 2). Measuring donor emission before (Fig. 2A,D) and after photo-bleaching of the YFP (Fig. 2B,E) revealed a normalized FRET efficiency of 19.3 ± 2.5% ($n = 13$) for the CFP–YFP and 30.9 ± 2.4% ($n = 11$) for the GFP2–YFP pair (Fig. 2C,F). Thus the FRET efficiency obtained for GFP2–YFP is 60% higher as compared to CFP–YFP, consistent with the predicted efficiency increase of 58% derived from the spectral data (Fig. 1C). Control experiments co-expressing CFP or GFP2 together with the YFP did not result in any detectable FRET signal (data not shown). The increased FRET efficiency of the GFP2–YFP pair could also be confirmed by donor photo-bleaching [18] (data not shown), which was simplified by the large separation of GFP2 and YFP excitation. In contrast, for the CFP–YFP pair FRET measurements by donor photo-bleaching were difficult to achieve due to photo-bleaching of the YFP acceptor by the 457 nm excitation light used for bleaching CFP (not shown).

FRET measurements by acceptor or donor photo-bleaching are well suited for experiments in fixed cells, as the fluorescent molecules cannot move anymore during the bleaching procedure. To test the suitability of the GFP2–YFP FRET pair for its use in living cells, GFP2 and YFP were either co-transfected without a linker (Fig. 3A–D) or as the tandem construct (Fig. 3E–H) and FRET was determined by sensitized emission. No sensitized emission was observed in cells expressing GFP2 and YFP, but a clear FRET signal was detectable in cells expressing the tandem construct (compare Fig. 3B,F,D,H). No direct excitation of YFP was detectable above the background signal in the sample expressing donor and acceptor without a linker (Fig. 3B). Thus, the signal shown in Fig. 3F shows only sensitized emission due to FRET and is not caused by direct excitation of the acceptor.

In summary, we demonstrate here that spectral imaging and linear un-mixing extends the choice of FRET donor/acceptor pairs to those with high spectral overlap of donor emission and acceptor excitation. As demonstrated for the GFP2–YFP FRET pair this results in an increased FRET efficiency compared to the most commonly used FRET pair consisting of CFP and YFP. Because of the clear separation of donor and acceptor excitation in the GFP2–YFP pair, specific donor–acceptor interactions are detectable even in the presence of a high amount of non-interacting acceptors. Altogether, this allows the detection of FRET signals with increased sensitivity compared to the CFP–YFP pair. The algorithms used here for spectral un-mixing are simple and can easily be extended to different donor–acceptor pairs. Since the image acquisition equipment used is commercially available, the method is readily applicable.

Acknowledgements: We thank Dr. A. Squire for critical comments on the manuscript, Leica Microsystems (Mannheim, Germany) for continuous support to the ALMF and Brigitte Joggerst for excellent technical assistance. We also thank Stephan Geley for the GFP-tagged nuclear localization sequence construct and Patrick Keller for the cell line expressing tubulin–YFP.

References

[1] Förster, T. (1948) Ann. Phys. 2, 57–75.
[2] Pollock, B.A. and Heim, R. (1999) Trends Cell Biol. 9, 57–60.
[3] Heim, R. (1999) Methods Enzymol. 302, 408–423.
[4] Mahajan, N., Linder, K., Berry, G., Gordon, G.W., Heim, R. and Herman, B. (1998) Nat. Biotechnol. 16, 547–552.
[5] Heim, R. and Tsien, R.Y. (1996) Curr. Biol. 6, 178–182.
[6] Sato, M., Ozawa, T., Inukai, K., Asano, T. and Umezawa, Y. (2002) Nat. Biotechnol. 20, 287–294.
[7] Gordon, G.W., Berry, G., Liang, X.H., Levine, B. and Herman, B. (1998) Biophys. J. 74, 2702–2713.
[8] Simpson, J.C., Wellenreuther, R., Poustka, A., Pepperkok, R. and Wiemann, S. (2000) EMBO Rep. 1, 287–292.
[9] Girod, A., Kinzel, V. and Bossemeyer, D. (1996) FEBS Lett. 391, 121–125.
[10] Patterson, G., Day, R.N. and Piston, D. (2001) J. Cell. Sci. 114, 837–838.
[11] Lakowicz, J.R. (1999), Principles of Fluorescence Spectroscopy, Kluwer Academic/Plenum Publishers, New York.
[12] Herman, B. (1989) Methods Cell Biol. 30, 219–243.
[13] Wouters, F.S., Verveer, P.J. and Bastiaens, P.I.H. (2001) Trends Cell Biol. 11, 203–211.
[14] Nagai, T., Ibata, K., Park, E.S., Kubota, M., Mikoshiba, K. and Miyawaki, A. (2002) Nat. Biotechnol. 20, 87–90.
[15] Lansford, R., Bearman, G. and Fraser, S.E. (2001) J. Biomed. Opt. 6, 311–318.
[16] Dickinson, M.E., Bearman, G., Tilie, S., Lansford, R. and Fraser, S.E. (2001) BioTechniques 31, 1272–1278.
[17] Bastiaens, P.I.H. and Jovin, T.M. (1998) in: Cell Biology: A Laboratory Handbook (Celis, J.E., Ed.), Vol. 3, pp. 136–146, Academic Press, New York.
[18] Gadella Jr., T.W.J. and Jovin, T.M. (1995) J. Cell Biol. 129, 1543–1558.